MOLECULAR AND CELLULAR BIOLOGY, Aug. 2006, p. 5838–5849 Vol. 26, No. 15
0270-7306/06/$08.00+0 doi:10.1128/MCB.00556-06

CXCR3 Requires Tyrosine Sulfation for Ligand Binding and a Second Extracellular Loop Arginine Residue for Ligand-Induced Chemotaxis

Richard A. Colvin, Gabriele S. V. Campanella, Lindsay A. Manice, and Andrew D. Luster*

Center for Immunology and Inflammatory Diseases, Division of Rheumatology, Allergy, and Immunology, Massachusetts General Hospital, Boston, Massachusetts 02129

Received 29 March 2006/Accepted 7 May 2006

CXCR3 is a G-protein-coupled seven-transmembrane domain chemokine receptor that plays an important role in effector T-cell and NK cell trafficking. Three gamma interferon-inducible chemokines activate CXCR3: CXCL9 (Mig), CXCL10 (IP-10), and CXCL11 (I-TAC). Here, we identify extracellular domains of CXCR3 that are required for ligand binding and activation. We found that CXCR3 is sulfated on its N terminus and that sulfation is required for binding and activation by all three ligands. We also found that the proximal 16 amino acid residues of the N terminus are required for CXCL10 and CXCL11 binding and activation but not CXCL9 activation. In addition, we found that residue R216 in the second extracellular loop is required for CXCR3-mediated chemotaxis and calcium mobilization but is not required for ligand binding or ligand-induced CXCR3 internalization. Finally, charged residues in the extracellular loops contribute to the receptor-ligand interaction. These findings demonstrate that chemokine activation of CXCR3 involves both high-affinity ligand-binding interactions with negatively charged residues in the extracellular domains of CXCR3 and a lower-affinity receptor-activating interaction in the second extracellular loop. This lower-affinity interaction is necessary to induce chemotaxis but not ligand-induced CXCR3 internalization, further suggesting that different domains of CXCR3 mediate distinct functions.

Chemokines, or chemoattractant cytokines, are a family of small (8- to 10-kDa) secreted proteins that play an important role in the recruitment and activation of leukocytes (29). Approximately 50 chemokines have been described, and these chemokines interact with some redundancy with 20 G-protein-coupled chemokine receptors. The chemokine system, with its ability to control the migration of leukocytes, plays a critical role in both innate and adaptive immunity.

CXCR3 is a chemokine receptor that is expressed on the surface of a number of cell types, including activated $CD4^+$ and $CD8^+$ T cells, NK and NK-T cells, plasmacytoid dendritic cells, and some B cells (26, 27, 38, 45). CXCR3 is activated by three related chemokines: CXCL9, CXCL10, and CXCL11 (9, 26, 27, 38, 45). Each of these ligands is induced by gamma interferon and is produced in Th1-type immune responses (9, 14, 31). CXCR3 has been localized to infiltrating effector T cells in a wide variety of human inflammatory diseases, including atherosclerosis (32), rheumatoid arthritis (38), multiple sclerosis (3, 43), heart and lung transplant rejection (1, 22, 50), and psoriasis (17). The CXCR3 ligands have similarly been identified in these same lesions (1, 17, 20, 32, 36), leading to the hypothesis that this receptor-ligand system plays an important role in the recruitment of effector T cells into these lesions, resulting in T-cell-mediated inflammation. Supporting this hypothesis, CXCR3-deficient mice were protected from heart allograft transplant rejection and autoimmune type 1 diabetes mellitus in murine models (19, 23). Likewise, using CXCL10-deficient mice and inhibitory monoclonal antibodies, CXCL10 was shown to play a similar role in these same models (8, 22) as well as small bowel allograft rejection (48, 49) and the host response to *Toxoplasma gondii* and murine hepatitis virus (13, 24, 25). Together, these data support a critical role for both CXCR3 and its ligands in T-cell-mediated inflammation.

Our previous work has shown that the three CXCR3 ligands induce differential internalization of CXCR3 (10, 40). CXCL10- and CXCL9-induced internalization proceeds through the dynamin/β-arrestin 1 pathway, while CXCL11-induced CXCR3 endocytosis is dynamin and β-arrestin independent (10, 40). Additionally, we found that CXCL10- and CXCL9-induced CXCR3 internalization requires the C terminus of CXCR3, while CXCL11-induced CXCR3 internalization is independent of the C terminus and instead requires the third intracellular loop of CXCR3 (10). These data demonstrate that the different ligands of CXCR3 induce different downstream effects that may contribute to their biological differences.

Multiple receptor domains are required for chemokine-chemokine receptor interactions. CCL2 binds the CCR2 N terminus with high affinity and subsequently binds the second extracellular loop with lower affinity to induce receptor activation (34). Similarly, CXCL12 binds to the N terminus of CXCR4 and requires residues in the second extracellular domain to activate signaling (12). These results support a two-step mechanism of chemokine receptor activation similar to the model originally proposed for C5a receptor activation (42).

Posttranslational modifications have been shown to be important for chemokine receptor function. Tyrosine sulfation of the N termini of some chemokine receptors has been shown to be essential for chemokine binding and receptor activation (15, 16, 18, 21, 37). This posttranslational modification is also essential for human immunodeficiency virus type 1 entry through CCR5 and CXCR4 (16) and the binding of the Duffy antigen/

* Corresponding author. Mailing address: Center for Immunology and Inflammatory Diseases, Massachusetts General Hospital, 149 Thirteenth Street, Room 8031, Charlestown, MA 02129. Phone: (617) 726-5710. Fax: (617) 726-5651. E-mail: aluster@partners.org.

receptor of chemokines to the Duffy binding proteins of *Plasmodium* (7).

The roles of the extracellular domains of CXCR3 have previously been evaluated by analyzing the binding and function of chimeric CXCR3-CXCR1 receptors (47). In those studies, each of the extracellular domains played a role in the binding of the CXCR3 ligands, while the second extracellular loop was important for receptor activation (47).

To further analyze CXCR3 function, we have used site-directed mutagenesis of CXCR3 to systematically analyze each extracellular domain of CXCR3 and identify residues important for ligand binding and receptor activation. We determined that tyrosine sulfation of the N terminus is essential for activation by all three ligands and that a sulfated peptide corresponding to residues 18 to 37 of the CXCR3 N terminus inhibits CXCR3 function. Furthermore, we identified residue R216 in the second extracellular loop as essential for receptor activation but not for ligand binding or ligand-induced CXCR3 internalization. Finally, we found that charged residues in the extracellular loops contribute to ligand binding.

MATERIALS AND METHODS

Reagents. Recombinant human CXCL9, CXCL10, and CXCL11 were purchased from Peprotech (Rock Hill, NJ). The phycoerythrin (PE)-conjugated anti-CXCR3 antibody 1C6 was purchased from R&D Systems (Minneapolis, MN). The bovine-preprolactin-FLAG plasmid was a gift of Israel Charo (University of California at San Francisco). The retroviral expression vector pMigR and the packaging cell line Phoenix were gifts of Gary Nolan (Stanford University). Peptides corresponding to the CXCR3 N terminus were obtained from Synpep (Dublin, CA).

Cells. 300-19 cells are a murine pre-B-cell leukemia cell line that functionally expresses CXCR4 and, following transfection, can functionally express other chemokine receptors (2, 39). 300-19 cells were grown in complete RPMI medium containing 10% fetal bovine serum (FBS).

Plasmids and mutagenesis. All receptors used in this study are derived from human CXCR3. A cDNA encoding CXCR3 was inserted into the KpnI and EcoRI restriction sites in the multicloning site of pcDNA3.1 (Invitrogen, Carlsbad, CA). Point mutations were introduced into CXCR3 by using the QuikChange mutagenesis kit from Stratagene (La Jolla, CA) and oligonucleotides encoding the specific changes. The N-terminal truncation of CXCR3, V16-CXCR3, was constructed using a forward PCR primer starting at base 48 of the CXCR3 coding sequence. Chimeric genes encoding the bovine preprolactin signal sequence and the FLAG tag upstream of CXCR3 were constructed by ligating the preprolactin and FLAG genes to CXCR3 at a SalI site. Prolactin-FLAG (PF)-CXCR3 and PF-V16-CXCR3 were subcloned into the retroviral expression vector pMigR between the XhoI and EcoRI restriction sites. All constructs were sequenced bidirectionally.

Transfections. pcDNA3.1-based constructs were transfected stably into 300-19 cells by electroporation. 300-19 cells (1×10^7) were incubated with 10 μg of linearized CXCR3/pcDNA3.1 constructs for 10 min on ice and electroporated using a Bio-Rad (Hercules, CA) Gene Pulser II at 200 V and 1,000 mF in a 0.2-cm-gap electrode cuvette (Bio-Rad). Following electroporation, the cells were grown in RPMI medium containing 10% FBS for 24 h, at which time 80 μg/ml G418 (Mediatech) was added for selection.

Retroviral transductions. The ecotropic packaging cell line Phoenix was transiently transfected with PF-CXCR3 or PF-V16-CXCR3 in pMigR using Fugene 6 (Roche). The supernatants were collected 72 h after transfection and spun at 1,500 rpm for 10 min to remove any cells. Two hundred microliters of supernatant containing approximately 100,000 CFU per ml was added to 20,000 300-19 cells in the presence of 5 μg/ml Polybrene. The cells were spun for 90 min at 2,000 rpm. Forty-eight hours after infection, more than 90% of the cells were infected and expressed CXCR3.

Enrichment of CXCR3 or CXCR3 mutant-expressing cells. Transfected cells (5×10^6) were stained with 3 μl of the CXCR3 antibody 1C6 conjugated to PE (R&D Systems, Minneapolis, MN) in phosphate-buffered saline (PBS) containing 10% goat serum for 30 min at 4°C. The stained cells were washed and then incubated with microbeads coupled to an anti-PE antibody, and CXCR3-expressing cells were positively selected over a MACS LS column according to the manufacturer's protocol (Miltenyi Biotec, Auburn, CA). The positively selected cells were then cultured in complete RPMI medium without G418.

Cell surface and intracytoplasmic expression of CXCR3 and CXCR3 mutants. Cultured cells were resuspended in 100 μl of fluorescence-activated cell sorter buffer (PBS without calcium and magnesium) containing 1% bovine serum albumin (BSA), 0.1% sodium azide, and 10% goat serum. Cells were incubated for 5 min at room temperature. The anti-CXCR3 antibody 1C6, conjugated to PE or allophycocyanin (APC) (R&D Systems), was added to the cells, which were then incubated at 4°C for 30 min. For PF-V16-CXCR3 and PF-CXCR3, the anti-FLAG antibody M2 (Sigma) conjugated to biotin and streptavidin conjugated to APC were used to determine cell surface expression. The cells were washed twice in PBS and subsequently fixed by resuspension in PBS with 2% paraformaldehyde. Receptor cell surface expression was measured on a FACSCalibur flow cytometer (BD Biosciences, San Jose, CA), and the data were analyzed using FlowJo (Treestar, Ashland, OR). For total CXCR3 expression, cells were fixed in 2% paraformaldehyde, permeabilized using the Fix and Perm kit (Caltag, Burlingame, CA), stained with anti-CXCR3 antibody 1C6 conjugated to APC, and measured in a FACSCalibur flow cytometer, and the data were analyzed using FlowJo (Treestar).

Binding assays. Binding assays were performed as previously reported (6). Briefly, 400,000 wild-type or mutant CXCR3/300-19 cells were placed into 96-well tissue culture plates in a total volume of 150 μl of binding buffer (0.5% BSA, 5 mM $MgCl_2$, 1 mM $CaCl_2$, 50 mM HEPES, pH 7.4). A total of 0.04 nM of ^{125}I-labeled CXCL10 (New England Nuclear, Boston, MA) or CXCL11 (Amersham Biosciences, Piscataway, NJ) and 5×10^{-6} nM to 500 nM of unlabeled CXCL10 or CXCL11 (Peprotech, Rocky Hill, NJ) were added to the cells and incubated for 90 min at room temperature with shaking. The cells were transferred onto 96-well filter plates (Millipore, Billerica, MA) that were presoaked in 0.3% polyethyleneimine and washed three times with 200 μl binding buffer supplemented with 0.5 M NaCl. The plates were dried, and the radioactivity was measured after the addition of scintillation fluid in a Wallac Microbeta scintillation counter (Perkin-Elmer Life Sciences, Boston, MA). The data were analyzed using Grafit (Erithacus Software Ltd., Staines, United Kingdom). Each experiment was performed in duplicate and repeated at least twice.

Chemotaxis assays. Chemotaxis assays of 300-19 cells were performed in 96-well Neuroprobe chemotaxis chambers with 5-μm-pore-size polycarbonate membranes (Neuroprobe, Gaithersburg, MD) as previously reported (10). Thirty-one microliters of RPMI medium containing 1% BSA and chemokines was placed in the bottom chamber of the device according to the manufacturer's directions. About 25,000 cells were layered onto the top of the membrane in RPMI medium containing 1% BSA. The chambers were then incubated at 37°C for 5 h. The top of the filter was washed with deionized water, and the chambers were subjected to centrifugation at 1,500 rpm for 5 min. The filters were removed, and medium was aspirated. The chambers were then frozen at −80°C for at least 1 h. Twenty microliters of CyQuant dye mix (Molecular Probes, Eugene, OR) was added to each well of the Neuroprobe chamber. Following a 2-h incubation period, the fluorescence was measured using a CytoFluor fluorescent plate reader (Applied Biosystems, Foster City, CA). For each experiment, a cellular titration curve was completed to ensure that the fluorescence reading was in the linear range of the CyQuant dye, and the background fluorescence was subtracted from the readings for each sample. The chemotactic index was determined by dividing the fluorescence at each chemokine concentration by the fluorescence when no chemokine was added. Chemotaxis data were statistically analyzed using analysis of variance (ANOVA).

Calcium flux. Wild-type or mutant CXCR3/300-19 cells (5×10^6) were resuspended in 2 ml of RPMI medium with 1% BSA. Fifteen micrograms of Fura-2 (Molecular Probes, Eugene, OR) was added, and the cells were incubated at 37°C for 20 min. The cells were washed twice in PBS and resuspended in 2 ml of calcium flux buffer (145 mM NaCl, 4 mM KCl, 1 mM $NaHPO_4$, 1.8 mM $CaCl_2$, 25 mM HEPES, 0.8 mM $MgCl_2$, and 22 mM glucose). Fluorescence readings were measured at 37°C in a DeltaRAM fluorimeter (Photon Technology International, Lawrenceville, NJ). Before and after the addition of chemokines, intracellular calcium concentrations were recorded as the excitation fluorescence intensity emitted at 510 nm in response to sequential excitation at 340 nm and 380 nm and are presented as the relative ratio of fluorescence at 340 nm to that at 380 nm.

Internalization. Internalization assays were performed as previously reported (10). A total of 2.5×10^5 wild-type CXCR3/300-19 or mutant CXCR3/300-19 cells in RPMI medium with 1% BSA were incubated with various concentrations of CXCL10, CXCL11, or CXCL9 for 30 min at 37°C. Following the incubations, the cells were washed with ice-cold fluorescence-activated cell sorter buffer and subsequently analyzed for surface expression of CXCR3 using the PE-conjugated CXCR3 antibody 1C6 as described above.

TABLE 1. Expression, chemokine binding, and ligand-induced chemotaxis of CXCR3 and CXCR3 mutants[a]

Receptor	Conserved between human and mouse?	% WT surface expression on transfected 300-19 cells	CXCL10			CXCL11			% WT chemotaxis at 10 nM CXCL9
			IC_{50} (nM)	% WT binding	% WT chemotaxis at 1 nM CXCL10	IC_{50} (nM)	% WT binding	% WT chemotaxis at 10 nM CXCL11	
CXCR3	NA	100	0.062 ± 0.06	100	100	0.5 ± 0.138	100	100	100
V16	NA	248 ± 32	NC	12 ± 0	12.5 ± 2	NC	20 ± 28	15.7 ± 2	114 ± 18
Y27F	Y	106 ± 30	NC	0	20 ± 7	NA	NA	13 ± 17	1.1 ± 5
Y29F	Y	116 ± 50	NC	17 ± 3	10 ± 3	NA	NA	22 ± 4	1.1 ± 5
Y27FY29F	Y	94 ± 16	NC	0	12 ± 10	NA	NA	13 ± 8	6 ± 5
Y27AY29A	Y	107.5 ± 43	NC	0	0	NC	0	0	0
E4K	Y	140 ± 35	0.049 ± 0.16	85 ± 0.21	97 ± 4	1.2 ± 0.58	110 ± 21	97 ± 8	78 ± 15
E21K	Y	125 ± 64	0.108 ± 0.16	90 ± 0	58 ± 11	1.82 ± 2.1	75 ± 25	43 ± 6	142 ± 14
D112K	Y	100 ± 35	NC	0	2 ± 0.5	NC	0	0 ± 0.9	15 ± 9
D112A	Y	77.3 ± 8.3	NC	0	24 ± 7	NC	0	14 ± 3	14 ± 8
R197A	Y	128 ± 63	NC	0	3.7 ± 1	NC	0	8 ± 0.5	6 ± 0.4
R212A	Y	102 ± 7.5	NC	0	2.9 ± 0.6	NC	0	35 ± 5	18 ± 4
R216A	Y	121 ± 30	0.016	50	18 ± 5	1.35 ± 1.8	100 ± 10	13 ± 3	12 ± 4
D278K	Y	105 ± 10	NC	0	1.5 ± 6	NC	0	3 ± 4	2 ± 3
D278A	Y	40 ± 18	NC	0	35 ± 5	NC	0	0 ± 11	33 ± 5
D282K	Y	120 ± 30	NC	0	11 ± 6	NC	0	33 ± 7	27 ± 5
D282A	Y	47.5 ± 15	NC	20	13 ± 3	NC	0	13 ± 2	11 ± 2
E293K	Y	100 ± 14	NC	0	0 ± 1	NC	0	0 ± 1	0 ± 0.5
E293A	Y	137 ± 65	NC	20	1 ± 0.4	NC	0	41 ± 10	21 ± 3

[a] Surface expression and percent wild-type binding are expressed in comparison to wild-type CXCR3 expression and binding; means ± standard deviations are shown. % WT chemotaxis indicates the percentage of each mutants' chemotactic index compared to the wild-type CXCR3 chemotactic index at the peak ligand concentration. NC indicates that no IC_{50} value could be calculated. NA, data are not available; Y, yes.

Actin polymerization. A total of 1×10^5 wild-type CXCR3/300-19 or mutant CXCR3/300-19 cells in RPMI medium with 1% BSA were incubated with CXCL10, CXCL11, or CXCL9 (10 nM) for the indicated times at 37°C. Following the incubations, the cells were fixed with 2% paraformaldehyde, permeabilized with Fix and Perm (Caltag), and stained with phalloidin-APC (Molecular Probes). F-actin polymerization was subsequently measured by flow cytometry in a FACSCalibur flow cytometer, and the data were analyzed using FlowJo (Treestar). F-actin polymerization was determined by calculating the mean fluorescence index of the cells at each time point following stimulation with chemokine.

Sulfation. 300-19 cells (10×10^6) stably transfected with wild-type CXCR3 or Y27AY29A-CXCR3 were grown in minimal essential medium without sulfate and containing 10% FBS. A total of 500 μCi of [^{35}S]sulfate was added to each sample. Four hours later, the cells were washed in PBS, and cellular extracts were made. Briefly, cells were lysed in PBS containing 1% *n*-dodecyl-β-maltoside plus protease inhibitors. Following cell lysis, extracts were cleared by centrifugation, and proteins were immunoprecipitated using 3 μg of the monoclonal anti-CXCR3 antibody 1C6 (R&D Systems, Minneapolis, MN). Following overnight incubation at 4°C, the immunoprecipitates were captured using the Seize kit (Pierce, Rockford, IL) and resolved by 10% sodium dodecyl sulfate-polyacrylamide gel electrophoresis (SDS-PAGE). Gels were dried on a vacuum gel drier and subsequently exposed to autoradiography film for 24 h.

RESULTS

Tyrosine sulfation is required for CXCR3 function. Several chemokine receptors, notably, CCR5 and CXCR4, have been shown to be sulfated at tyrosine residues in their N termini. To explore the possibility that CXCR3 is sulfated, the amino acid sequence of CXCR3 was examined using an online computer program to identify potential tyrosine sulfation sites (28). The program determined that CXCR3 is likely sulfated at N-terminal residues Y27 and Y29. These residues are conserved between human and mouse CXCR3. We have found that both human and mouse CXCL9, CXCL10, and CXCL11 activate human and murine CXCR3 equivalently, suggesting the conservation of structure and function (data not shown).

To test the importance of these residues in CXCR3 ligand binding and function, CXCR3 mutants Y27F-CXCR3, Y29F-CXCR3, Y27FY29F-CXCR3, and Y27AY29A-CXCR3 were constructed. The sequence encoding tyrosines 27 and 29 was replaced with that encoding phenylalanines (Y27F-CXCR3, Y29F-CXCR3, and Y27FY29F-CXCR3) or alanines (Y27AY29A-CXCR3) using the QuikChange site-directed mutagenesis kit, and the cDNA was stably transfected into 300-19 B cells. Total and extracellular expression of Y27F-CXCR3, Y29F-CXCR3, Y27FY29F-CXCR3, and Y27AY29A-CXCR3 was similar to wild-type CXCR3 expression (Table 1 and data not shown). CXCL10 and CXCL11 binding to Y27FY29F-CXCR3 and Y27AY29A-CXCR3 was not detected (Table 1). CXCL9 binding assays were not performed, as there is no commercially available ^{125}I-labeled preparation of this chemokine, and we were unable to obtain biologically active ^{125}I-labeled CXCL9 or Alexa-labeled CXCL9.

CXCL10, CXCL9, and CXCL11 were tested for their ability to induce chemotaxis of Y27FY29F-CXCR3/300-19 cells. These chemokines induced no significant chemotaxis of these cells (Fig. 1). The ability of CXCL10, CXCL9, and CXCL11 to induce calcium mobilization in Y27AY29A-CXCR3 was also tested. No calcium signal was seen following stimulation with these chemokines, although a robust signal was apparent following CXCL12 stimulation of the same cells (data not shown). Furthermore, CXCL10-, CXCL9-, and CXCL11-induced Y27FY29F-CXCR3 internalization was significantly reduced compared to that of wild-type CXCR3 (Table 2). These data demonstrate that despite a high level of cell surface expression, Y27FY29F-CXCR3 does not bind CXCL10, CXCL9, or CXCL11, and these chemokines did not bind or induce signaling through this mutant receptor.

To further delineate the relative importance of Y27 and Y29 for CXCR3 tyrosine sulfation and ligand interactions, phenylalanine was substituted for Y27 and Y29 individually (Table 1). CXCL10 binding was not detected on Y27F-CXCR3/300-19 cells (Table 1). CXCL10 binding was reduced significantly on

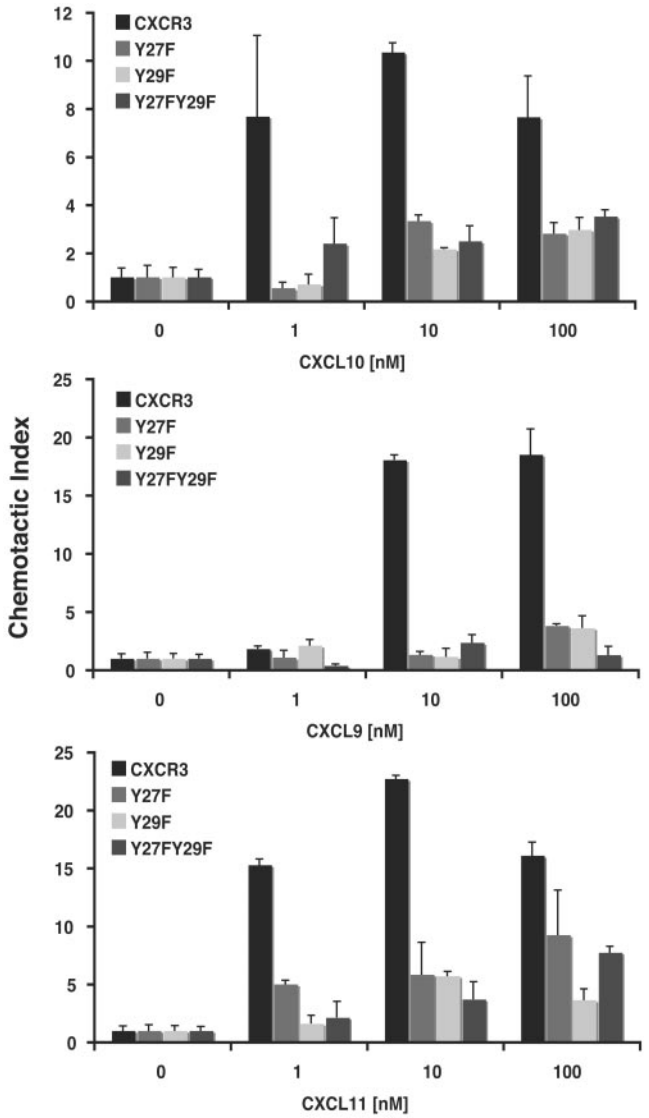

FIG. 1. Chemotaxis in cells expressing CXCR3 N-terminal tyrosine mutations. Wild-type CXCR3 and Y27F-, Y29F-, Y27FY29F-, andY27AY29A-CXCR3/300-19 cells were activated by CXCL10, CXCL9, and CXCL11. (A) Chemotaxis. The bars represent the migration of wild-type CXCR3/300-19, Y27F-CXCR3/300-19, Y29F-CXCR3/300-19, or Y27FY29F-CXCR3/300-19 cells across a Neuroprobe membrane to CXCL10, CXCL9, or CXCL11. The *x* axis represents the chemokine concentration (nanomolar), and the *y* axis represents the chemotactic index. The data shown are the means of two samples, and the experiment shown is representative of three similar experiments. Data were compared using two-way ANOVA. For each of the mutant receptors, the curve was shifted significantly with a *P* value of <0.01.

Y29F-CXCR3/300-19 cells. Due to the low level of chemokine binding in the absence of competitor (~20% of wild-type CXCR3 for CXCL10), a 50% inhibitory concentration (IC_{50}) value could not be determined for CXCL10–Y29F-CXCR3 binding. Migration of Y27F-CXCR3/300-19 and Y29F-CXCR3/300-19 cells to the CXCR3 ligands was reduced to background levels (Fig. 1). These data suggest that both Y27 and Y29 are required for the induction of chemotaxis by CXCL9, CXCL10, or CXCL11.

To determine if residues Y27 and/or Y29 were sulfated, wild-type CXCR3, Y27F-, Y29F-, and Y27FY29F-CXCR3/300-19 cells were incubated with sodium [^{35}S]sulfate for 4 h. An aliquot from each of the cell cultures demonstrated that these receptors were expressed similarly to wild-type CXCR3 (Fig. 2A). Cell lysates were immunoprecipitated using the anti-CXCR3 antibody 1C6 and analyzed by SDS-PAGE (Fig. 2B). Only wild-type CXCR3 and Y29F were detectable following labeling with [^{35}S]sulfate. The signal intensity of Y29F-CXCR3 was approximately one-half of that of wild-type CXCR3. Y27F-CXCR3 and Y27FY29F were not detectable. These data demonstrate that CXCR3 is sulfated and that Y27 is sulfated preferentially over Y29. It is likely that Y29 is also sulfated on wild-type CXCR3 but that sulfation at this position requires a tyrosine at position 27. A similar phenomenon was shown for the stepwise sulfation of the four N-terminal tyrosines of CCR5 (41). Of note, the ^{35}S-labeled CXCR3 migrated at approximately 70 kDa, similar to our previously published results that showed that ^{32}P-labeled CXCR3 and unlabeled CXCR3 identified by Western blotting also migrated at 70 kDa (10).

A sulfated peptide representing the N-terminal sequence around tyrosines 27 and 29 inhibits ligand activation of CXCR3. To further test the importance of tyrosine sulfation in CXCR3 function, we synthesized two peptides from CXCR3 amino acid residues 18 through 37. In the sulfated peptide, tyrosines 27 and 29 were sulfated, while in the sulfate-free peptide, the tyrosines were left unsulfated. Chemotaxis experiments were performed to determine if these peptides could inhibit CXCR3-mediated chemotaxis. As shown in Fig. 3, at 100 nM, 1 μM, and 10 μM, the sulfated peptide inhibited CXCR3-mediated chemotaxis to CXCL10 and CXCL11, while the unsulfated peptide did not inhibit CXCL10 or CXCL11 chemotaxis (Fig. 3). Neither peptide affected the migration of CXCR3/300-19 cells to CXCL12 (data not shown). These data demonstrate that a peptide corresponding to the CXCR3 N terminus can act as an inhibitor of CXCR3 function and that this inhibition requires sulfation at Y27 and/or Y29.

The proximal 16 amino acids of CXCR3 are required for CXCL10 and CXCL11 binding. The N terminus of several chemokine receptors has been shown to play an important role in chemokine binding (4, 34). In order to determine the role of the N terminus of CXCR3 in chemokine binding and signaling, a mutant, called PF-V16-CXCR3, in which the proximal 16

TABLE 2. Receptor internalization

Receptor	% of mutant CXCR3 compared to WT ± SD[a]			
	Y27FY29F	R197A	R216A	D278A
CXCL10	15 ± 2.2**	36 ± 10**	95 ± 8.7	45 ± 8.6**
CXCL9	12 ± 7.3**	44 ± 8.5**	146 ± 2.9*	63 ± 5.0*
CXCL11	52 ± 4.5**	65 ± 7.6**	120 ± 6.1**	65 ± 9.6**

[a] Percentage of mutant CXCR3 compared to wild-type CXCR3 receptor internalization ± standard deviation following stimulation with CXCL10, CXCL9, or CXCL11. Wild-type CXCR3/300-19 or mutant CXCR3/300-19 cells were stimulated with 100 nM CXCL10, 200 nM CXCL9, or 10 nM CXCL11 for 15 min at 37°C. Internalization was calculated by comparing receptor expression in the presence of chemokine to receptor expression in the absence of chemokine at 15 min. *, the internalization difference was statistically significant compared to that of wild-type CCR3 at a *P* value of <0.05 using Student's *t* test; **, the internalization difference was statistically significant compared to that of wild-type CXCR3 at a *P* value of <0.01 using Student's *t* test.

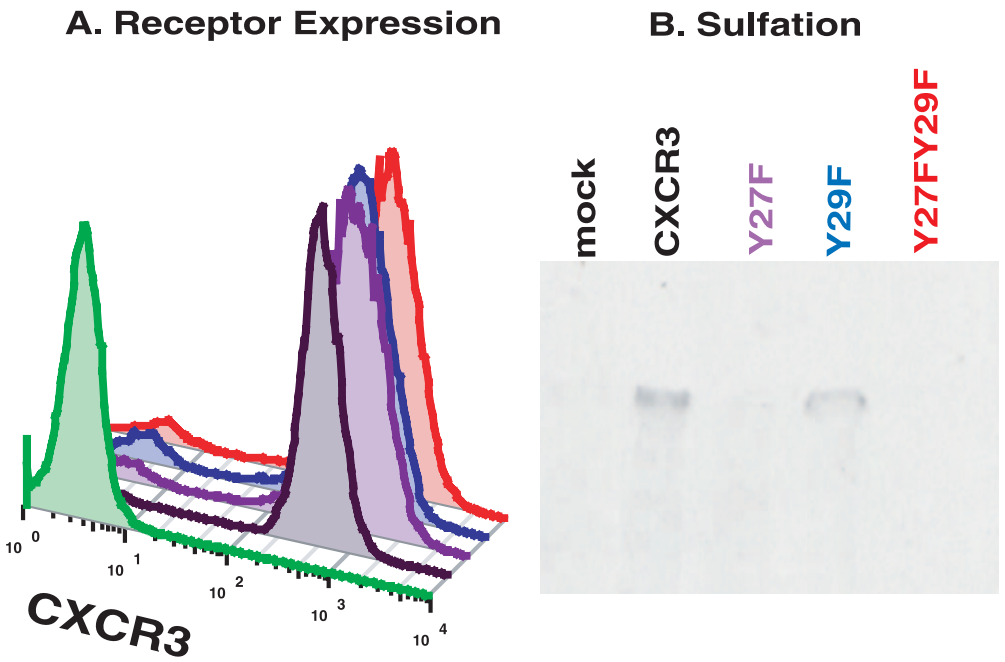

FIG. 2. Tyrosine sulfation of CXCR3. Wild-type CXCR3, Y27F-CXCR3, Y29F-CXCR3, and Y27FY29F-CXCR3/300-19 cells were incubated for 4 h with [^{35}S]sulfate. (A) Cell surface expression of wild-type CXCR3, Y27F-CXCR3, Y29F-CXCR3, and Y27FY29F-CXCR3. Following incubation with [^{35}S]sulfate, an aliquot of cells was stained with anti-CXCR3 antibody 1C6 conjugated to APC and analyzed by flow cytometry for CXCR3 or CXCR3 mutant receptor cell surface expression. The *x* axis represents CXCR3 expression, and the *y* axis represents the percentage of cells. The green line represents mock-transfected 300-19 cells, the black line represents wild-type CXCR3/300-19 cells, the purple line represents Y27F-CXCR3/300-19 cells, the blue line represents Y29F-CXCR3/300-19 cells, and the red line represents Y27FY29F-CXCR3/300-19 cells. (B) Immunoprecipitation of ^{35}S-labeled CXCR3 or CXCR3 mutants as indicated. The cells were incubated for 4 h with [^{35}S]sulfate, lysed, and subsequently immunoprecipitated with anti-CXCR3 antibody 1C6. Immunoprecipitations were analyzed using SDS-PAGE. CXCR3 migrated at 70 kDa.

amino acids of CXCR3 were deleted was constructed. V16-CXCR3 is not recognized by anti-CXCR3 antibody 1C6 (data not shown). In order to detect V16-CXCR3 by flow cytometry, a prolactin signal sequence and FLAG tag were cloned in frame onto the 5′ end of this cDNA, as well as that of wild-type CXCR3, to allow for the detection of cell surface expression using antibodies to the FLAG epitope. The PF-V16-CXCR3 cDNA was cloned into pcDNA3.1 and stably transfected into 300-19 cells. PF-CXCR3 and PF-V16-CXCR3 cDNAs were then subcloned into pMigR. Retroviral particles were produced and used to transduce 300-19 cells. Following retroviral transduction, PF-V16-CXCR3 was expressed at slightly higher levels than PF-CXCR3 (Table 1). Due to the low level of chemokine binding to PF-V16 in the absence of competitor (~12% of PF-CXCR3 for CXCL10 and ~20% of PF-CXCR3 for CXCL11), no IC_{50} value for PF-V16-CXCR3/300-19 cell binding to CXCL10 and CXCL11 could be calculated (Table 1).

PF-V16-CXCR3/300-19 cells were significantly diminished in their ability to migrate to CXCL10 and CXCL11 but not CXCL9 (Fig. 4A). The peak chemotactic index for migration of PF-V16-CXCR3/300-19 cells to CXCL10 was 50% of that for PF-CXCR3/300-19 cells, and the dose of CXCL10 required to induce significant chemotaxis was 100-fold higher for PF-V16-CXCR3/300-19 cells than for PF-CXCR3/300-19 cells (Fig. 4A). CXCL11-induced chemotaxis of PF-V16-CXCR3/300-19 cells required a 10-fold-higher dose to achieve a similar chemotactic index as that in PF-CXCR3/300-19 cells (Fig. 4A). These differences were statistically significant at a *P* value of <0.01 using ANOVA. There was no significant change in CXCL9-induced chemotaxis of PF-V16-CXCR3/300-19 cells compared to that of PF-CXCR3/30019 cells. Consistent with the chemotaxis data, there was no detectable calcium mobilization following CXCL10 stimulation, minimal calcium mobilization following CXCL11 stimulation, and robust calcium mobilization in PF-V16-CXCR3/300-19 cells following CXCL9 stimulation (Fig. 4B). Similarly, the polymerization of F-actin was not observed following CXCL10 or CXCL11 stimulation of PF-V16-CXCR3/300-19 cells. In contrast, CXCL9 induced the polymerization of F-actin similarly in PF-V16-CXCR3/300-19 and wild-type CXCR3/300-19 cells (Fig. 4C). These data, generated from three different assays for receptor function, suggest that the first 16 amino acids of CXCR3 are important for maximal CXCL10 and CXCL11 binding and activation but are dispensable for CXCL9 activation.

Acidic residues in the amino terminus are not critical for CXCR3 function. The CXCR3 ligands are all positively charged, and it has been shown that a single basic residue, R8, of CXCL10 is essential for CXCR3 binding (6). We sought to determine if charged residues in the CXCR3 N terminus were important for interactions with its ligands. We chose to examine charged residues, E4 and E21, in the N terminus that are conserved between murine and human CXCR3 to further analyze the role of this domain in chemokine binding and activation. Lysine was substituted for these residues, thereby reversing the charge of the residue from negative to positive.

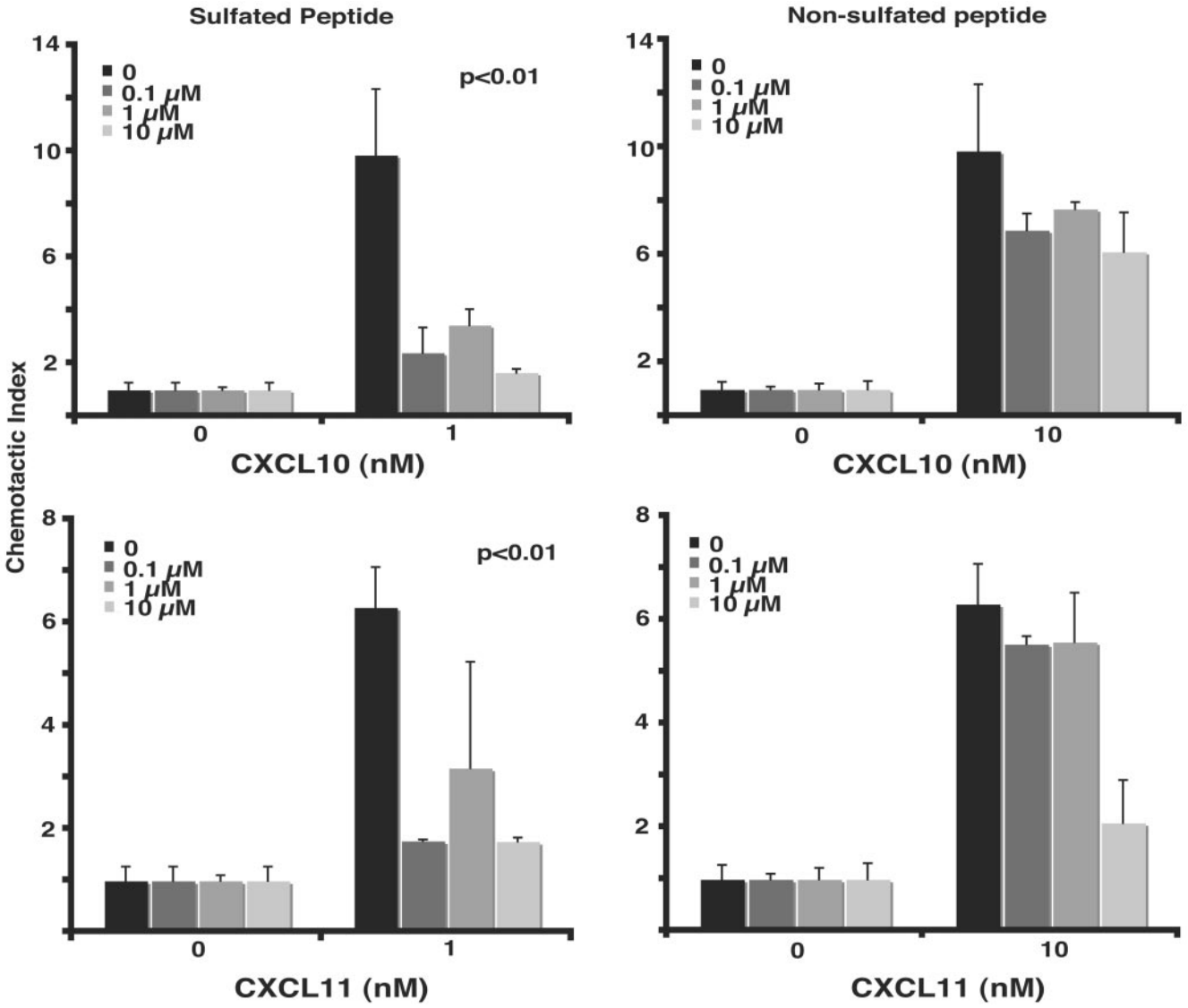

FIG. 3. Inhibition of CXCR3-mediated chemotaxis by a sulfated N-terminal peptide of CXCR3. Sulfated (tyrosine residues 27 and 29) and nonsulfated peptides corresponding to amino acid residues 18 to 37 of the N terminus of CXCR3 were synthesized. Chemokines were combined with peptides at the indicated concentrations. Migration of wild-type CXCR3/300-19 cells across the Neuroprobe membrane in response to CXCL10, CXCL11, and CXCL12 at the indicated concentrations in the presence or absence of the peptides at the indicated concentrations was measured. The data shown are the means of two samples, and the experiment shown is representative of four similar experiments.

Following stable transfection of E4K-CXCR3 into 300-19 cells, cell surface expression was similar to that of wild-type CXCR3 (Table 1). CXCL10 and CXCL11 bound E4K-CXCR3/300-19 cells similarly to wild-type CXCR3/300-19 cells in the absence of any competitor (Table 1). The IC_{50} values for CXCL10 and CXLC11 binding to E4K-CXCR3/300-19 cells were not statistically different from those of wild-type CXCR3/300-19 cells (Table 1). Functionally, chemotaxis following CXCL10, CXCL9, and CXCL11 stimulation was slightly diminished for E4K-CXCR3/300-19 cells compared to that for wild-type CXCR3/300-19 cells (Table 1). Calcium mobilization following CXCL10, CXCL9, and CXCL11 stimulation, however, was similar for E4K-CXCR3/300-19 cells and wild-type CXCR3/300-19 cells (data not shown). These data suggest that residue E4 is not required for CXCL10, CXCL9, and CXCL11 binding and function.

E21K was also introduced into the CXCR3 N terminus. Following stable transfection of E21K-CXCR3 into 300-19 cells, cell surface expression was similar to that of wild-type CXCR3 (Table 1). CXCL10 and CXCL11 bound E21K-CXCR3/300-19 cells similarly to wild-type CXCR3/300-19 cells in the absence of any competitor (Table 1). The IC_{50} values for CXCL10 and CXLC11 binding to E21K-CXCR3/300-19 cells were not statistically different from those of wild-type CXCR3/300-19 cells (Table 1). Chemotaxis induced by CXCL10, CXCL9, and CXCL11 was slightly diminished for E21K-CXCR3/

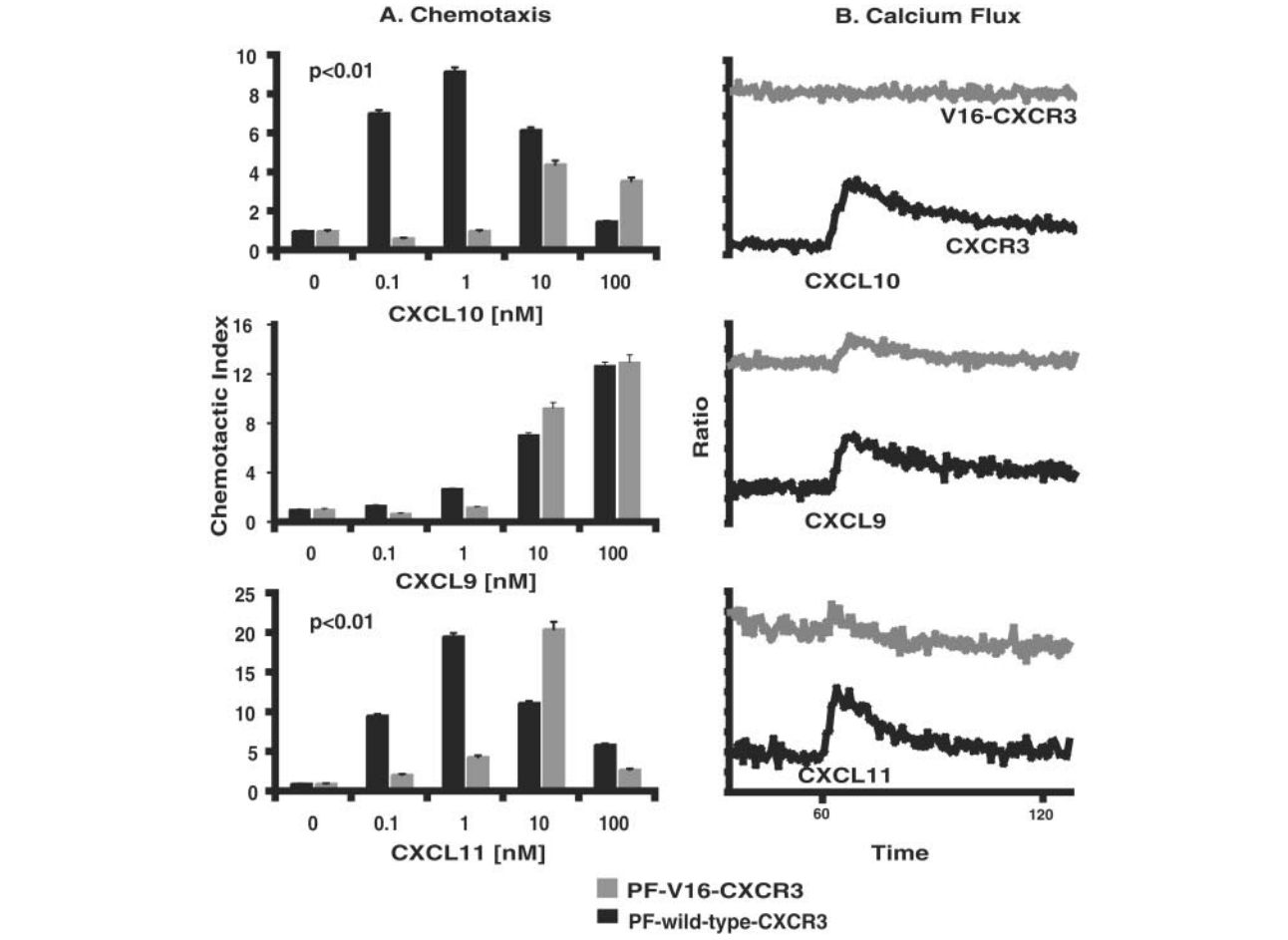
A. Chemotaxis
B. Calcium Flux
p<0.01
CXCL10 [nM]
Chemotactic Index
CXCL9 [nM]
p<0.01
CXCL11 [nM]
V16-CXCR3
CXCR3
CXCL10
Ratio
CXCL9
CXCL11
Time
PF-V16-CXCR3
PF-wild-type-CXCR3

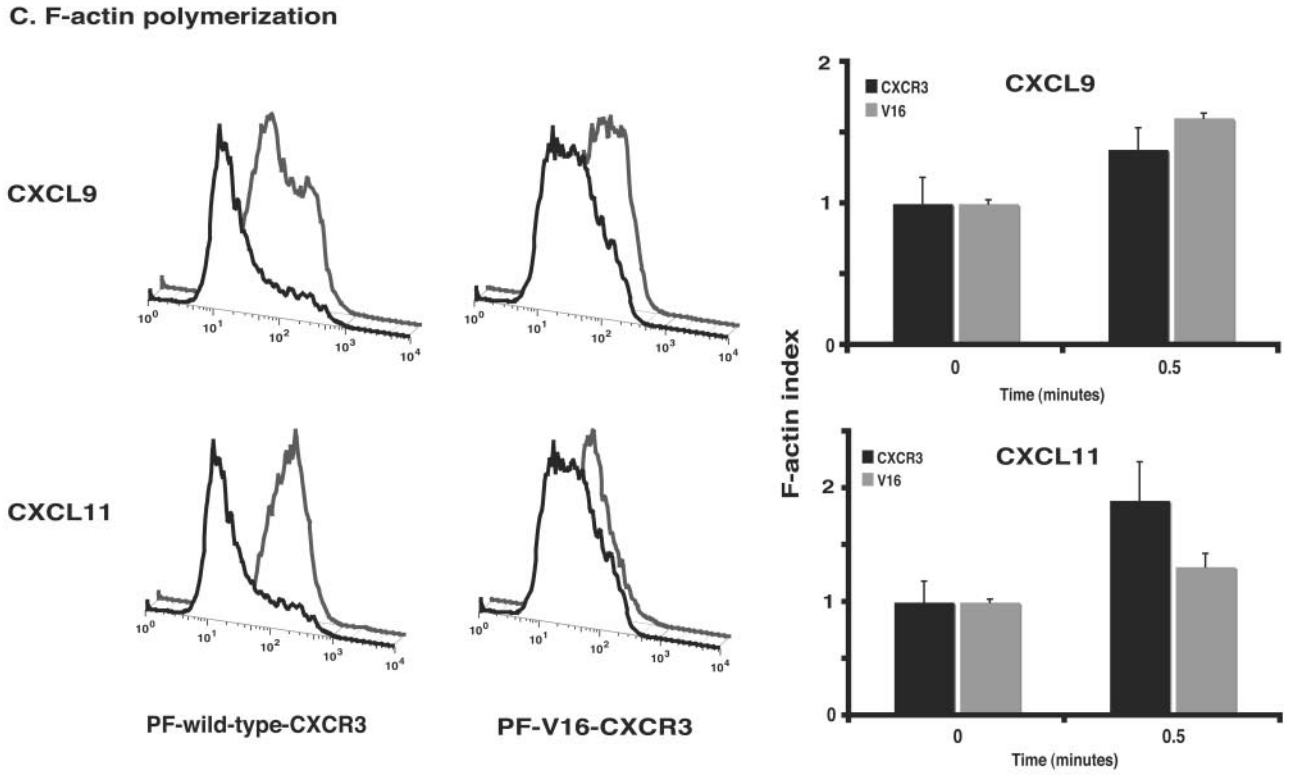
C. F-actin polymerization
CXCL9
CXCL11
PF-wild-type-CXCR3
PF-V16-CXCR3
CXCR3
V16
F-actin index
Time (minutes)

300-19 cells compared to that for wild-type CXCR3/300-19 cells (Table 1). Calcium mobilization following CXCL10, CXCL9, and CXCL11 stimulation, however, was similar for E21K-CXCR3/300-19 cells and wild-type CXCR3/300–19cells (data not shown). These data suggest that E21 has a minimal role in CXCR3 function.

R216 in the second extracellular loop is required for CXCR3 activation. There are three conserved basic residues in the second extracellular loop of CXCR3: R197, R212, and R216. To determine the role of these residues in CXCR3 ligand binding and receptor function, alanines were substituted for each of these residues, and 300-19 cells expressing the mutant receptors were analyzed.

Following stable transfection of pcDNA3.1, encoding R216A-CXCR3, into 300-19 cells, the receptor was expressed similarly to wild-type CXCR3 (Table 1). CXCL10 and CXCL11 bound R216A-CXCR3/300-19 cells similarly to wild-type CXCR3/300-19 cells (Table 1). CXCL10-, CXCL9-, and CXCL11-induced chemotaxis of R216A-CXCR3/300-19 cells was significantly reduced compared to that of wild-type CXCR3/300-19 cells (Fig. 5). There was only minimal calcium flux following CXCL10 or CXCL11 stimulation and no calcium flux following CXCL9 stimulation of R216A-CXCR3/300-19 cells (Fig. 5). These data demonstrate that while R216 plays a minimal role in ligand binding, it plays a major role in the activation of chemotaxis.

Internalization of R216A-CXCR3. To further dissect the role of R216 in CXCR3 function, receptor internalization assays were performed. CXCL10-induced R216A-CXCR3 internalization was indistinguishable from wild-type CXCR3 internalization, while CXCL9- and CXCL11-induced R216A-CXCR3 internalization was slightly enhanced compared to that of wild-type CXCR3 (Table 2). In contrast, ligand-induced internalization of mutant CXCR3 receptors that have diminished ligand binding was significantly diminished compared to ligand-induced wild-type CXCR3 and R216A-CXCR3 internalization (Table 2). These results demonstrate that while R216 plays an important role in activating chemotaxis and calcium mobilization, it plays no role in facilitating receptor internalization.

R197 and R212. R197A-CXCR3 and R212A-CXCR3 were expressed similarly to wild-type CXCR3 on 300-19 cells (Table 1). No detectable CXCL10 or CXCL11 binding to R197A-CXCR3 was observed (Table 1). There was no significant detectable chemotaxis following CXCL10, CXCL9, or CXCL11 stimulation of R197A-CXCR3/300-19 cells (Table 1). Although calcium mobilization of the cells expressing mutated

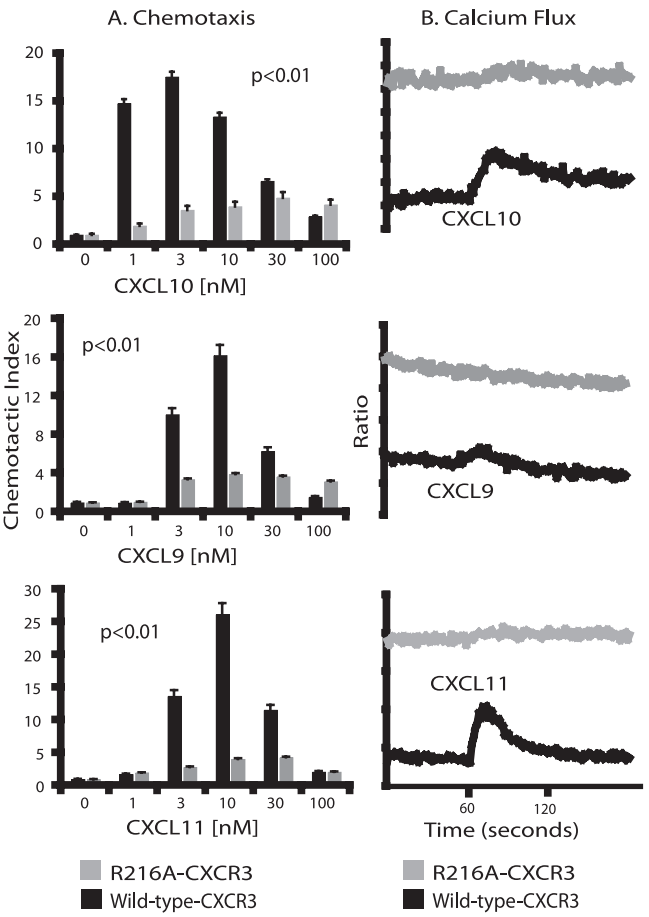

FIG. 5. R216A-CXCR3-mediated chemotaxis and calcium mobilization. Wild-type CXCR3/300-19 and R216A-CXCR3/300-19 cells were activated by CXCL10, CXCL9, and CXCL11. (A) Chemotaxis. The bars represent the migration of wild-type CXCR3/300-19 cells (black bars) or mutant CXCR3/300-19 cells (gray bars) across a Neuroprobe membrane to CXCL10, CXCL9, or CXCL11. The *x* axis represents the chemokine concentration (nanomolar), and the *y* axis represents the chemotactic index. The data shown are the means of two samples, and the experiment shown is representative of four similar experiments. Data were compared using two-way ANOVA. For significant shifts in the chemotaxis curves, *P* values are indicated in the figure. (B) Calcium mobilization. Wild-type CXCR3/300-19 or R216A-CXCR3/300-19 cells were loaded with Fura-2 and activated with 10 nM CXCL10, CXCL9, or CXCL11 at 60 s as indicated. The curves show the ratios of the 510-nm emissions after activation at 340 nm and 380 nm. The plots are representative of five experiments. Simultaneously, wild-type CXCR3/300-19 cells were stimulated by CXCL10, CXCL9, or CXCL11 and CXCL12 with curves similar to those shown in Fig. 1 (data not shown).

FIG. 4. PF-V16-CXCR3-mediated chemotaxis and calcium mobilization. Wild-type PF-CXCR3/300-19 and PF-V16-CXCR3/300-19 cells were activated by CXCL10, CXCL9, and CXCL11. (A) Chemotaxis. The bars represent the migration of wild-type PF-CXCR3/300-19 cells (black bars) or PF-V16-CXCR3/300-19 cells (gray bars) across a Neuroprobe membrane to CXCL10, CXCL9, or CXCL11. The *x* axis represents the chemokine concentration (nanomolar), and the *y* axis represents the chemotactic index. The data shown are the means of two samples, and the experiment shown is representative of five similar experiments. Data were compared using two-way ANOVA. For significant shifts in the chemotaxis curves, *P* values are indicated in the figure. (B) Calcium mobilization. Wild-type PF-CXCR3/300-19 and PF-V16-CXCR3/300-19 cells were loaded with Fura-2 and activated with 10 nM CXCL10, CXCL9, or CXCL11 at 60 s as indicated. The curves show the ratio of the 510-nm emissions after activation at 340 nm and 380 nm. The plots are representative of three experiments. (C) F-actin polymerization. Wild-type PF-CXCR3/300-19 cells or PF-V16-CXCR3-CXCR3/300-19 cells were activated with CXCL10, CXCL9, or CXCL11 (10 nM) for the indicated times. The activated cells were stained for F-actin polymerization with phalloidin-APC and analyzed by flow cytometry. The left-hand panels show representative histogram plots of F-actin staining of PF-wild-type-CXCR3 or PF-V16-CXCR3. The black curves represent F-actin staining in the absence of chemokine, and the red curves represent F-actin staining following the addition of 10 nM CXCL10 or CXCL11 for 30 s. The data shown in the bar graphs are the mean fluorescence indices of two samples, and the experiment shown is representative of three similar experiments.

CXCR3 was normal following CXCL12 stimulation, there was no detectable calcium mobilization following CXCL10, CXCL9, or CXCL11 stimulation (data not shown). Ligand-induced R197A-CXCR3 internalization was significantly diminished compared to wild-type CXCR3 internalization (Table 2). There was no significant detectable chemotaxis following CXCL10 or CXCL9 stimulation of R212A-CXCR3/300-19 cells, although at 10 nM CXCL11, minimal chemotaxis was found (Table 1 and data not shown). There was no detectable calcium mobilization following CXCL10, CXCL9, or CXCL11 stimulation (data not shown). These results suggest a role for R197 and R212 in CXCR3 binding to CXCL10, CXCL9, and CXCL11.

The first and third extracellular loops. In order to determine the role of the conserved charged residues in the first and third extracellular loops of CXCR3, substitutions were introduced, changing these residues to either lysine or alanine. The charged residues included D112, D278, D282, and E293. In each case, the mutant receptors were expressed similarly to wild-type CXCR3 on the cell surface of 300-19 cells (Table 1). No significant CXCL10 or CXCL11 binding to the mutant CXCR3/300-19 cells was observed (Table 1). Similarly, the ability of the CXCR3 ligands to activate each of these receptors was dramatically reduced (Table 1). Substitutions at D112 and D278 dramatically reduced CXCR3 function (Table 1 and data not shown). Substitution mutations at positions D282 and E293 similarly abrogated CXCL10 and CXCL9 activity but did not completely eliminate CXCL11 activity (Table 1). These results suggest that D112 and D278 are important for binding and activation by all three CXCR3 ligands, while D282 and E293 are important for activation by CXCL9 and CXCL10 but are less important for CXCL11 activation.

To exclude the possibility that differences in receptor function could be a result of differential metabolism and trafficking through cellular compartments, we measured total and cell surface wild-type CXCR3 and mutant CXCR3 expression in stably transfected 300-19 cells. We found that there were no significant differences in the ratio of cell surface to total receptor expression between wild-type CXCR3 and any of the mutant receptors studied (data not shown). These data make it less likely that altered intracellular trafficking of the mutant receptors is responsible for the observed phenotypes.

DISCUSSION

Insights into the mechanism of chemokine receptor activation offer clues into targets for interfering with cell trafficking. In this study, we explored the contributions of each of the extracellular domains of CXCR3, an inflammatory chemokine receptor found predominantly on T cells, in ligand binding and receptor function. We constructed mutants of human CXCR3 at predominantly charged residues that are conserved between human and murine CXCR3. Cell lines stably expressing similar levels of wild-type and mutant CXCR3 receptors were established, thereby facilitating direct comparisons of the binding and function of these receptors.

In summary, our data show that all four of the extracellular domains of CXCR3 are important for binding to its ligands and support a model of CXCR3 binding that requires ligand interactions with at least one sulfated tyrosine in the N terminus and receptor activation that requires an interaction with amino acid residue R216 in the second extracellular loop (Fig. 6).

Tyrosine sulfation is critical for CXCR3 function. Our data using tyrosine substitution mutants and sulfated and nonsulfated CXCR3 N-terminal peptides highlight the importance of CXCR3 sulfation for binding its ligands. Of note, tyrosines 27 and 29 are conserved between murine, human, rat, cow, and goat CXCR3 (28, 35, 46). Despite revealing the importance of tyrosine sulfation at CXCR3 residues Y27 and Y29, our data do not rule out the possibility of other potentially important posttranslational modifications near these residues. To date, five other chemokine receptors have been reported to be sulfated on their N termini: CXCR4, CCR2, CCR5, CCR8, and CX3CR1 as well as the Duffy antigen receptor for chemokines (Table 3) (7, 15, 16, 18, 21, 37). Sulfation of these receptors has been shown to be essential for chemokine binding and, in the case of CCR5 and CXCR4, for their function as human immunodeficiency virus type 1 coreceptors. Additionally, by using a computer program that identifies potential tyrosine sulfation sites (33) to analyze the sequences of all of the known chemokine receptors, we found that CXCR6, CCR1, and CCR10 may also contain sulfated residues in their N termini (Table 3). Together, these data show that tyrosine sulfation is a common posttranslational modification of C-C, C-X-C, and C-X-X-X-C chemokine receptors. It is notable that the receptors that have been shown to be sulfated, or are predicted to be sulfated, are generally considered lymphocyte chemokine receptors. In contrast, those that are considered granulocyte chemokine receptors have not been shown or predicted to be sulfated. One possible explanation for this observation is that lymphocytes have fewer heparan sulfate proteoglycan chemokine binding sites on their surface than other leukocytes (30, 44). Sulfation of lymphocyte chemokine receptors may compensate for the relative paucity of negatively charged glycosaminoglycans on the lymphocyte cell surface and allow basic chemokines to dock with the receptor's N terminus prior to activating the receptor through the second extracellular loop.

Our data also demonstrate that a sulfated peptide corresponding to the CXCR3 N terminus around tyrosines 27 and 29 can block CXCR3-mediated chemotaxis. Previously, a peptide corresponding to the N terminus of CX3CR1 has been shown to bind CX3CL1 (fractalkine) only when sulfated; however, inhibition of CX3CL1 function by the sulfated peptide was not shown (18). To our knowledge, our study is the first report showing that a sulfated synthetic peptide corresponding to the N terminus of a chemokine receptor can inhibit chemokine receptor function. These data suggest that a sulfated peptidomimetic small molecule inhibitor may be useful as a pharmacological agent to block CXCR3 function.

CXCR3 activation is a two-step mechanism. Our data show that CXCL10, CXCL9, and CXCL11 bind the N terminus of CXCR3 at the sulfated tyrosine residues. These chemokines also require additional interactions in the first and third extracellular loops of CXCR3 for stable binding. CXCL10 and CXCL11 further require the proximal N terminus for stable binding. Following high-affinity binding of these chemokines to CXCR3, they then interact with R216 in the second extracellular loop to activate the receptor. A similar model of a two-step mechanism for chemokine binding and activation has been proposed for other chemokine receptors (34, 42). Our

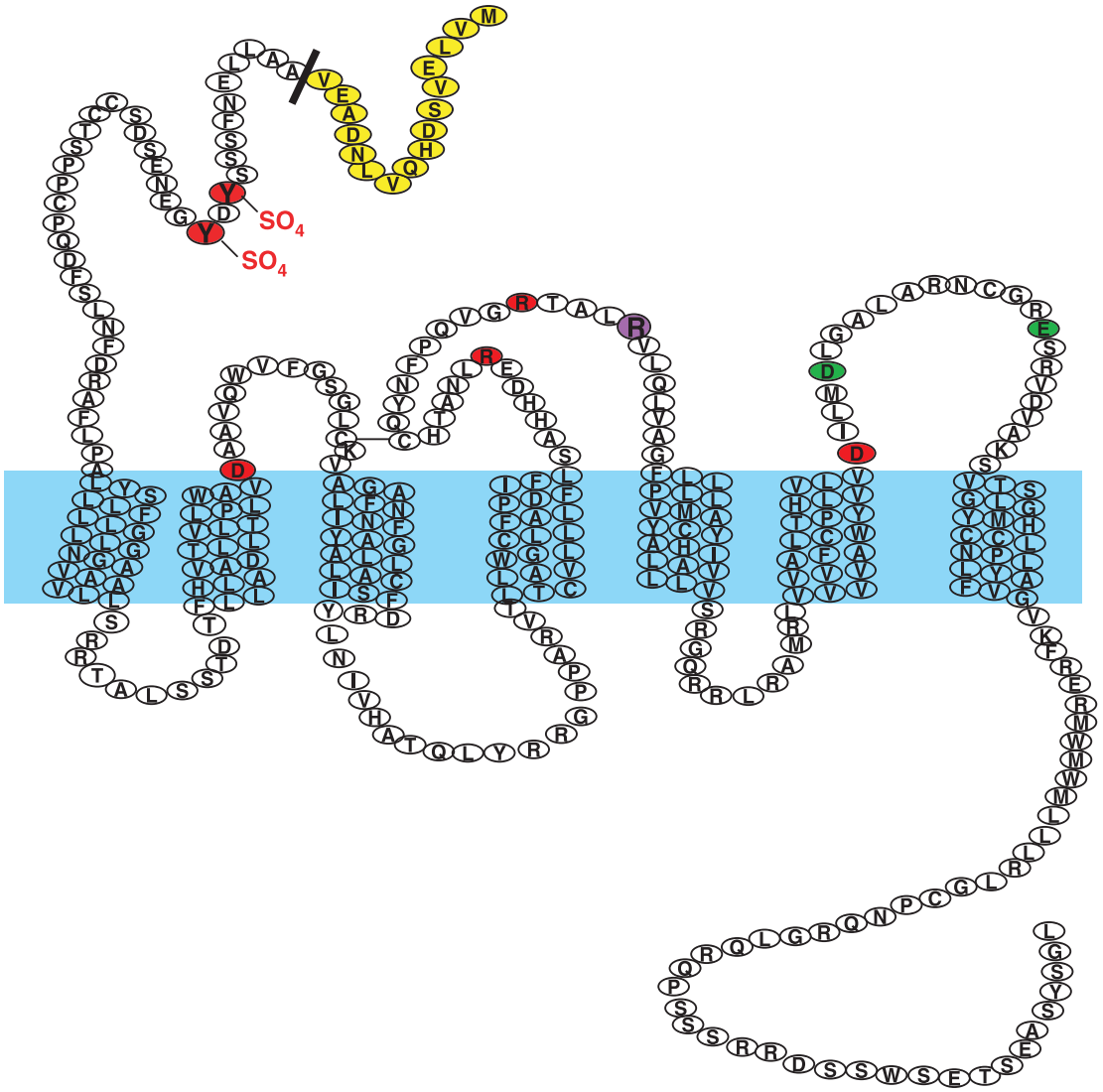

FIG. 6. CXCR3 residues important for ligand binding and activation. Residues highlighted in red were required for CXCL9, CXCL10, and CXCL11 binding. Residues in yellow were required only for CXCL10 and CXCL11 binding, while residues in green were required only for CXCL9 and CXCL10 binding. Residue R216, highlighted in purple, was required for CXCL9-, CXCL10-, and CXCL11-induced CXCR3-mediated chemotaxis but not for ligand binding or receptor internalization.

TABLE 3. Chemokine receptors that are known or predicted to be sulfated at their N termini

Receptor	Predicted sulfation site(s)	Predominant cell type(s)[a]	Reference or source
CXCR3	Y27, Y29	Th1-activated T cells, NK cells, monocytes	This study
CXCR4	Y21	Lymphocytes	15
CXCR6	Y6	Activated T cells, NK T cells	None
CCR1	Y10, Y18	Monocytes, activated T cells	None
CCR2	Y26, Y28	Monocytes, macrophages	37
CCR5	Y3, Y10, Y14, Y15	Th1-activated T cells, monocytes, DCs	16
CCR8	Y2	T cells in the thymus, Th2-activated T cells	21
CCR10	Y23, Y24, Y25, Y27	Activated T cells, B cells	None
CX3CR1	Y14	Monocytes, DCs, T cells, NKT cells	18
DARC	Y30, Y41	RBCs	7

[a] DCs, dendritic cells; RBCs, red blood cells.

data demonstrate that the second step of CXCR3 activation is not required to induce receptor internalization, suggesting that the mechanisms of chemotaxis and receptor internalization are separable. Previously, we have shown that there are two distinct mechanisms of CXCR3 internalization: CXCL10- and CXCL9-induced internalization proceeds through a β-arrestin 1- and C terminus-dependent pathway, while CXCL11-induced CXCR3 internalization requires the third intracellular loop of CXCR3 and proceeds independently of β-arrestin 1 and 2 and the C terminus (10). Activation of CXCR3 through R216 is not important to induce CXCR3 internalization through either of these pathways. In contrast to the activation of chemotaxis and calcium mobilization, we have not identified any specific residues or domains that are essential for the induction of CXCR3 internalization apart from those required for high-affinity ligand binding.

Charged residues in CXCR3 are essential for interactions with its ligands. We have previously shown that positively charged residues in CXCL10 are essential for CXCR3 binding and activation (6). Furthermore, CXCL9 and CXCL11 are also positively charged ligands, suggesting that CXCR3-ligand interactions may be based in large part on charge. The data in our present study show that the negatively charged conserved residues in the first and third extracellular domains of CXCR3 are important in ligand binding and activation. Substitutions of the positively charged residues R197 and R212 in the second extracellular loop resulted in a receptor that did not bind any of the CXCR3 ligands or mediate chemotaxis or calcium flux following ligand stimulation. R197 and R212 clearly have a distinct role from R216 in CXCR3 function. Data from the loss-of-function CXCR3 substitution mutations cannot distinguish direct interactions of charged residues with ligands from disruptions in the structure of CXCR3. All of the mutant receptors reported are recognized on the cell surface by 1C6, a monoclonal antibody raised against the CXCR3 N terminus, suggesting that the N terminus and the first *trans*-membrane domain of these mutants are intact. Furthermore, CXCL11 can partially activate D282A-CXCR3 and E293-CXCR3, suggesting that these receptors have an intact structure.

It has been suggested that the CXCR3-CXCL10 interaction results from hydrophobic interactions (5). However, in that study, important interactions based on charge would not be observed because CXCR3 was represented by a nonsulfated N-terminal peptide consisting of residues 22 through 42. Furthermore, the peptide-CXCL10 K_d was measured to be 2 μM, which is at least 1,000-fold higher than the K_d for the CXCR3-CXCL10 interaction (11). While hydrophobic interactions may play a role in the CXCR3-CXCL10 interaction, our data support an essential role for charged residues for the interaction of CXCL10, as well as CXCL9 and CXCL11, with full-length cell surface-expressed CXCR3.

CXCR3 domain exchange experiments. Previously, a molecular characterization of the CXCR3 extracellular domains was undertaken using domain-swapping experiments whereby the extracellular domains of CXCR3 were exchanged with those of CXCR1 (47). In this model, the CXCR3 N terminus was shown to be important for CXCL10 and CXCL11 binding, and the second extracellular loop was shown to be important for receptor activation. Our data confirm and extend that study significantly, as we now identify specific residues in all four extracellular domains that are required for ligand binding and identify the specific residue in the second extracellular loop required for receptor activation.

In summary, the N terminus of CXCR3 is sulfated, and that sulfation is required for binding and activation by all three ligands. In addition, negatively charged residues in the first and third extracellular domains of CXCR3 contribute to ligand binding. Furthermore, while R216 in the second extracellular domain plays no role in CXCL10 or CXCL11 binding or ligand-induced internalization, this residue is required for the activation of chemotaxis by all three CXCR3 ligands. These data suggest a model in which sulfated tyrosines and negatively charged residues play an important role in tethering the basic CXCR3 ligands to the receptor. Once bound to CXCR3, the ligands must interact with R216 to activate the receptor to induce chemotaxis. These insights into CXCR3 ligand binding and activation may be helpful in designing inhibitors specifically targeting CXCR3-mediated inflammation.

ACKNOWLEDGMENTS

This work was supported by NIH grant K08 AI50147 and a Harvard Center for AIDS Research fellowship to R.A.C. and NIH grants PO1 DK50305, R01 DK07449, and R01 CA69212 to A.D.L.

REFERENCES

1. **Agostini, C., F. Calabrese, F. Rea, M. Facco, A. Tosoni, M. Loy, G. Binotto, M. Valente, L. Trentin, and G. Semenzato.** 2001. Cxcr3 and its ligand CXCL10 are expressed by inflammatory cells infiltrating lung allografts and mediate chemotaxis of T cells at sites of rejection. Am. J. Pathol. **158:**1703–1711.
2. **Alt, F., N. Rosenberg, S. Lewis, E. Thomas, and D. Baltimore.** 1981. Organization and reorganization of immunoglobulin genes in A-MULV-transformed cells: rearrangement of heavy but not light chain genes. Cell **27:**381–390.
3. **Balashov, K. E., J. B. Rottman, H. L. Weiner, and W. W. Hancock.** 1999. CCR5(+) and CXCR3(+) T cells are increased in multiple sclerosis and their ligands MIP-1alpha and IP-10 are expressed in demyelinating brain lesions. Proc. Natl. Acad. Sci. USA **96:**6873–6878.
4. **Blanpain, C., B. J. Doranz, A. Bondue, C. Govaerts, A. De Leener, G. Vassart, R. W. Doms, A. Proudfoot, and M. Parmentier.** 2003. The core domain of chemokines binds CCR5 extracellular domains while their amino terminus interacts with the transmembrane helix bundle. J. Biol. Chem. **278:**5179–5187.
5. **Booth, V., D. W. Keizer, M. B. Kamphuis, I. Clark-Lewis, and B. D. Sykes.** 2002. The CXCR3 binding chemokine IP-10/CXCL10: structure and receptor interactions. Biochemistry **41:**10418–10425.
6. **Campanella, G. S., E. M. Lee, J. Sun, and A. D. Luster.** 2003. CXCR3 and heparin binding sites of the chemokine IP-10 (CXCL10). J. Biol. Chem. **278:**17066–17074.
7. **Choe, H., M. J. Moore, C. M. Owens, P. L. Wright, N. Vasilieva, W. Li, A. P. Singh, R. Shakri, C. E. Chitnis, and M. Farzan.** 2005. Sulphated tyrosines mediate association of chemokines and Plasmodium vivax Duffy binding protein with the Duffy antigen/receptor for chemokines (DARC). Mol. Microbiol. **55:**1413–1422.
8. **Christen, U., D. B. McGavern, A. D. Luster, M. G. von Herrath, and M. B. Oldstone.** 2003. Among CXCR3 chemokines, IFN-gamma-inducible protein of 10 kDa (CXC chemokine ligand (CXCL) 10) but not monokine induced by IFN-gamma (CXCL9) imprints a pattern for the subsequent development of autoimmune disease. J. Immunol. **171:**6838–6845.
9. **Cole, K. E., C. A. Strick, T. J. Paradis, K. T. Ogborne, M. Loetscher, R. P. Gladue, W. Lin, J. G. Boyd, B. Moser, D. E. Wood, B. G. Sahagan, and K. Neote.** 1998. Interferon-inducible T cell alpha chemoattractant (I-TAC): a novel non-ELR CXC chemokine with potent activity on activated T cells through selective high affinity binding to CXCR3. J. Exp. Med. **187:**2009–2021.
10. **Colvin, R. A., G. S. Campanella, J. Sun, and A. D. Luster.** 2004. Intracellular domains of CXCR3 that mediate CXCL9, CXCL10, and CXCL11 function. J. Biol. Chem. **279:**30219–30227.
11. **Cox, M. A., C. H. Jenh, W. Gonsiorek, J. Fine, S. K. Narula, P. J. Zavodny, and R. W. Hipkin.** 2001. Human interferon-inducible 10-kDa protein and human interferon-inducible T cell alpha chemoattractant are allotopic ligands for human CXCR3: differential binding to receptor states. Mol. Pharmacol. **59:**707–715.
12. **Doranz, B. J., M. J. Orsini, J. D. Turner, T. L. Hoffman, J. F. Berson, J. A. Hoxie, S. C. Peiper, L. F. Brass, and R. W. Doms.** 1999. Identification of CXCR4 domains that support coreceptor and chemokine receptor functions. J. Virol. **73:**2752–2761.
13. **Dufour, J. H., M. Dziejman, M. T. Liu, J. H. Leung, T. E. Lane, and A. D. Luster.** 2002. IFN-gamma-inducible protein 10 (IP-10; CXCL10)-deficient mice reveal a role for IP-10 in effector T cell generation and trafficking. J. Immunol. **168:**3195–3204.
14. **Farber, J. M.** 1990. A macrophage mRNA selectively induced by gamma-interferon encodes a member of the platelet factor 4 family of cytokines. Proc. Natl. Acad. Sci. USA **87:**5238–5242.
15. **Farzan, M., G. J. Babcock, N. Vasilieva, P. L. Wright, E. Kiprilov, T. Mirzabekov, and H. Choe.** 2002. The role of post-translational modifications of the CXCR4 amino terminus in stromal-derived factor 1 alpha association and HIV-1 entry. J. Biol. Chem. **277:**29484–29489.
16. **Farzan, M., T. Mirzabekov, P. Kolchinsky, R. Wyatt, M. Cayabyab, N. P. Gerard, C. Gerard, J. Sodroski, and H. Choe.** 1999. Tyrosine sulfation of the amino terminus of CCR5 facilitates HIV-1 entry. Cell **96:**667–676.
17. **Flier, J., D. M. Boorsma, P. J. van Beek, C. Nieboer, T. J. Stoof, R. Willemze, and C. P. Tensen.** 2001. Differential expression of CXCR3 targeting chemokines CXCL10, CXCL9, and CXCL11 in different types of skin inflammation. J. Pathol. **194:**398–405.

18. **Fong, A. M., S. M. Alam, T. Imai, B. Haribabu, and D. D. Patel.** 2002. CX3CR1 tyrosine sulfation enhances fractalkine-induced cell adhesion. J. Biol. Chem. **277:**19418–19423.
19. **Frigerio, S., T. Junt, B. Lu, C. Gerard, U. Zumsteg, G. A. Hollander, and L. Piali.** 2002. Beta cells are responsible for CXCR3-mediated T-cell infiltration in insulitis. Nat. Med. **8:**1414–1420.
20. **Gottlieb, A. B., A. D. Luster, D. N. Posnett, and D. M. Carter.** 1988. Detection of a gamma interferon-induced protein IP-10 in psoriatic plaques. J. Exp. Med. **168:**941–948.
21. **Gutierrez, J., L. Kremer, A. Zaballos, I. Goya, A. C. Martinez, and G. Marquez.** 2004. Analysis of post-translational CCR8 modifications and their influence on receptor activity. J. Biol. Chem. **279:**14726–14733.
22. **Hancock, W. W., W. Gao, V. Csizmadia, K. L. Faia, N. Shemmeri, and A. D. Luster.** 2001. Donor-derived IP-10 initiates development of acute allograft rejection. J. Exp. Med. **193:**975–980.
23. **Hancock, W. W., B. Lu, W. Gao, V. Csizmadia, K. Faia, J. A. King, S. T. Smiley, M. Ling, N. P. Gerard, and C. Gerard.** 2000. Requirement of the chemokine receptor CXCR3 for acute allograft rejection. J. Exp. Med. **192:**1515–1520.
24. **Khan, I. A., J. A. MacLean, F. S. Lee, L. Casciotti, E. DeHaan, J. D. Schwartzman, and A. D. Luster.** 2000. IP-10 is critical for effector T cell trafficking and host survival in Toxoplasma gondii infection. Immunity **12:** 483–494.
25. **Liu, M. T., B. P. Chen, P. Oertel, M. J. Buchmeier, D. Armstrong, T. A. Hamilton, and T. E. Lane.** 2000. The T cell chemoattractant IFN-inducible protein 10 is essential in host defense against viral-induced neurologic disease. J. Immunol. **165:**2327–2330.
26. **Loetscher, M., B. Gerber, P. Loetscher, S. A. Jones, L. Piali, I. Clark-Lewis, M. Baggiolini, and B. Moser.** 1996. Chemokine receptor specific for IP10 and mig: structure, function, and expression in activated T-lymphocytes. J. Exp. Med. **184:**963–969.
27. **Loetscher, M., P. Loetscher, N. Brass, E. Meese, and B. Moser.** 1998. Lymphocyte-specific chemokine receptor CXCR3: regulation, chemokine binding and gene localization. Eur. J. Immunol. **28:**3696–3705.
28. **Lu, B., A. Humbles, D. Bota, C. Gerard, B. Moser, D. Soler, A. D. Luster, and N. P. Gerard.** 1999. Structure and function of the murine chemokine receptor CXCR3. Eur. J. Immunol. **29:**3804–3812.
29. **Luster, A. D.** 1998. Chemokines—chemotactic cytokines that mediate inflammation. N. Engl. J. Med. **338:**436–445.
30. **Luster, A. D., S. M. Greenberg, and P. Leder.** 1995. The IP-10 chemokine binds to a specific cell surface heparan sulfate site shared with platelet factor 4 and inhibits endothelial cell proliferation. J. Exp. Med. **182:**219–231.
31. **Luster, A. D., and J. V. Ravetch.** 1987. Biochemical characterization of a gamma interferon-inducible cytokine (IP-10). J. Exp. Med. **166:**1084–1097.
32. **Mach, F., A. Sauty, A. S. Iarossi, G. K. Sukhova, K. Neote, P. Libby, and A. D. Luster.** 1999. Differential expression of three T lymphocyte-activating CXC chemokines by human atheroma-associated cells. J. Clin. Investig. **104:**1041–1050.
33. **Monigatti, F., E. Gasteiger, A. Bairoch, and E. Jung.** 2002. The Sulfinator: predicting tyrosine sulfation sites in protein sequences. Bioinformatics **18:** 769–770.
34. **Monteclaro, F. S., and I. F. Charo.** 1997. The amino-terminal domain of CCR2 is both necessary and sufficient for high affinity binding of monocyte chemoattractant protein 1. Receptor activation by a pseudo-tethered ligand. J. Biol. Chem. **272:**23186–23190.
35. **Nagaoka, K., H. Nojima, F. Watanabe, K. T. Chang, R. K. Christenson, S. Sakai, and K. Imakawa.** 2003. Regulation of blastocyst migration, apposition, and initial adhesion by a chemokine, interferon gamma-inducible protein 10 kDa (IP-10), during early gestation. J. Biol. Chem. **278:**29048–29056.
36. **Patel, D. D., J. P. Zachariah, and L. P. Whichard.** 2001. CXCR3 and CCR5 ligands in rheumatoid arthritis synovium. Clin. Immunol. **98:**39–45.
37. **Preobrazhensky, A. A., S. Dragan, T. Kawano, M. A. Gavrilin, I. V. Gulina, L. Chakravarty, and P. E. Kolattukudy.** 2000. Monocyte chemotactic protein-1 receptor CCR2B is a glycoprotein that has tyrosine sulfation in a conserved extracellular N-terminal region. J. Immunol. **165:**5295–5303.
38. **Qin, S., J. B. Rottman, P. Myers, N. Kassam, M. Weinblatt, M. Loetscher, A. E. Koch, B. Moser, and C. R. Mackay.** 1998. The chemokine receptors CXCR3 and CCR5 mark subsets of T cells associated with certain inflammatory reactions. J. Clin. Investig. **101:**746–754.
39. **Roos, R. S., M. Loetscher, D. F. Legler, I. Clark-Lewis, M. Baggiolini, and B. Moser.** 1997. Identification of CCR8, the receptor for the human CC chemokine I-309. J. Biol. Chem. **272:**17251–17254.
40. **Sauty, A., R. A. Colvin, L. Wagner, S. Rochat, F. Spertini, and A. D. Luster.** 2001. CXCR3 internalization following T cell-endothelial cell contact: preferential role of IFN-inducible T cell alpha chemoattractant (CXCL11). J. Immunol. **167:**7084–7093.
41. **Seibert, C., M. Cadene, A. Sanfiz, B. T. Chait, and T. P. Sakmar.** 2002. Tyrosine sulfation of CCR5 N-terminal peptide by tyrosylprotein sulfotransferases 1 and 2 follows a discrete pattern and temporal sequence. Proc. Natl. Acad. Sci. USA **99:**11031–11036.
42. **Siciliano, S. J., T. E. Rollins, J. DeMartino, Z. Konteatis, L. Malkowitz, G. Van Riper, S. Bondy, H. Rosen, and M. S. Springer.** 1994. Two-site binding of C5a by its receptor: an alternative binding paradigm for G protein-coupled receptors. Proc. Natl. Acad. Sci. USA **91:**1214–1218.
43. **Sorensen, T. L., M. Tani, J. Jensen, V. Pierce, C. Lucchinetti, V. A. Folcik, S. Qin, J. Rottman, F. Sellebjerg, R. M. Strieter, J. L. Frederiksen, and R. M. Ransohoff.** 1999. Expression of specific chemokines and chemokine receptors in the central nervous system of multiple sclerosis patients. J. Clin. Investig. **103:**807–815.
44. **Stellrecht, C. M., W. M. Mars, H. Miwa, M. Beran, and G. F. Saunders.** 1991. Expression pattern of a hematopoietic proteoglycan core protein gene during human hematopoiesis. Differentiation **48:**127–135.
45. **Thomas, S. Y., R. Hou, J. E. Boyson, T. K. Means, C. Hess, D. P. Olson, J. L. Strominger, M. B. Brenner, J. E. Gumperz, S. B. Wilson, and A. D. Luster.** 2003. CD1d-restricted NKT cells express a chemokine receptor profile indicative of Th1-type inflammatory homing cells. J. Immunol. **171:**2571–2580.
46. **Wang, X., X. Li, D. B. Schmidt, J. J. Foley, F. C. Barone, R. S. Ames, and H. M. Sarau.** 2000. Identification and molecular characterization of rat CXCR3: receptor expression and interferon-inducible protein-10 binding are increased in focal stroke. Mol. Pharmacol. **57:**1190–1198.
47. **Xanthou, G., T. J. Williams, and J. E. Pease.** 2003. Molecular characterization of the chemokine receptor CXCR3: evidence for the involvement of distinct extracellular domains in a multi-step model of ligand binding and receptor activation. Eur. J. Immunol. **33:**2927–2936.
48. **Zhang, Z., L. Kaptanoglu, W. Haddad, D. Ivancic, Z. Alnadjim, S. Hurst, D. Tishler, A. D. Luster, T. A. Barrett, and J. Fryer.** 2002. Donor T cell activation initiates small bowel allograft rejection through an IFN-gamma-inducible protein-10-dependent mechanism. J. Immunol. **168:**3205–3212.
49. **Zhang, Z., L. Kaptanoglu, Y. Tang, D. Ivancic, S. M. Rao, A. Luster, T. A. Barrett, and J. Fryer.** 2004. IP-10-induced recruitment of CXCR3 host T cells is required for small bowel allograft rejection. Gastroenterology **126:** 809–818.
50. **Zhao, D. X., Y. Hu, G. G. Miller, A. D. Luster, R. N. Mitchell, and P. Libby.** 2002. Differential expression of the IFN-gamma-inducible CXCR3-binding chemokines, IFN-inducible protein 10, monokine induced by IFN, and IFN-inducible T cell alpha chemoattractant in human cardiac allografts: association with cardiac allograft vasculopathy and acute rejection. J. Immunol. **169:**1556–1560.